



Global Teleconnections between Pacific and Atlantic Ocean Surface Temperature Variability and Regional Hydrologic Cycle

Xiaoya Zhang, Hyungjun Kim, Taikan Oki

Graduate School of Arts and Sciences, The University of Tokyo, Tokyo, Japan

Institute of Industrial Science, The University of Tokyo, Tokyo, Japan

Integrated Research System for Sustainability Science, The University of Tokyo, Tokyo, Japan

Background

Global distribution of primary climate signals that drives precipitation and river discharge (Fig.1) (J D.Milliman et al. 2011)

River can response to positive/negative ENSO,NAO,PDO,AMO and SAM* indices

*Southern Annular Mode , aka Antarctic Oscillation

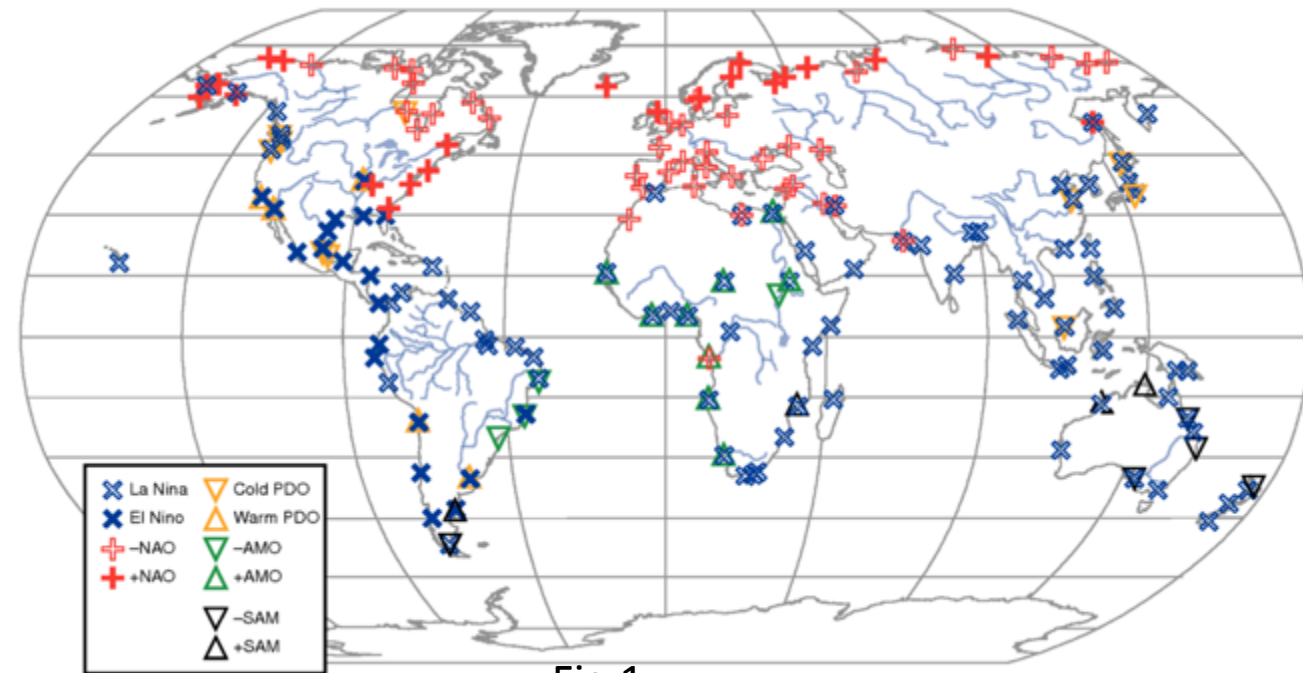


Fig.1

ONI &PDO are significantly anti-correlated with similarly smoothed variations of total terrestrial monthly mean runoff(Kim, H. 2017)

Correlations between the global freshwater discharge and ENSO are significant for the rivers draining to the Atlantic ($R = -0.5$ with Niño3.4), Pacific ($R = -0.61$), and Indian ($R = -0.52$) Oceans (Dai et al. 2009).

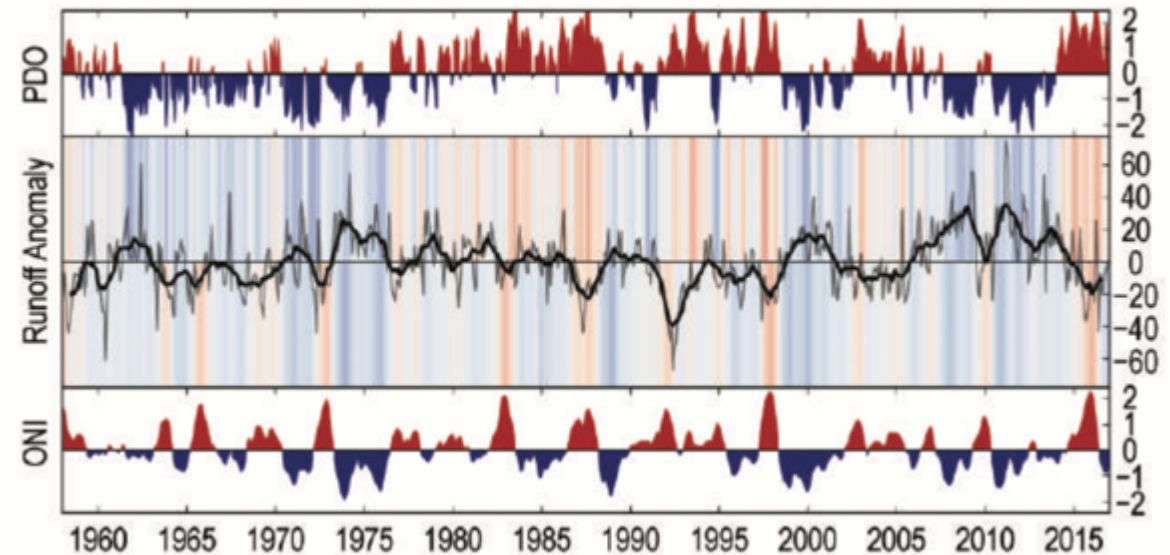
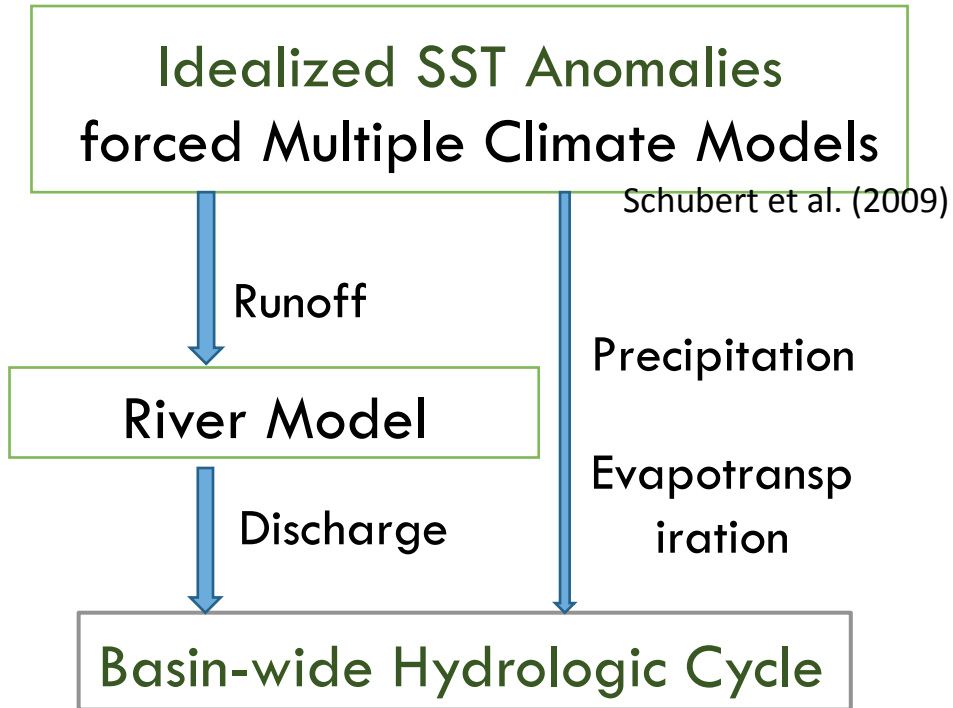


Fig.2 59-year series of total terrestrial runoff anomalies along with the ONI and PDO index smoothed by a 12-month running mean (Kim, H. 2017)

Teleconnection patterns Retrieval Scheme



Questions:

How global major rivers' discharge anomalies are related with ocean SST? What is the role of the different ocean basins?

Objectives:

To quantify strength of different ocean basins' impact in each river basin.

Dataset

US- Climate Variability and Predictability (CLIVAR) Drought working Group's Experiments

Assessment of the impact on drought processes by evaluation of multiple model simulations that address the roles of **sea surface temperature forcings**

- 5 climate models, 50 years simulation; forced with one or more of the idealized SST anomaly patterns;
- The leading patterns of SST variability are isolated by Rotated EOF methods from the monthly observation SST data 1901–2004 produced by Rayner et al. (2003).

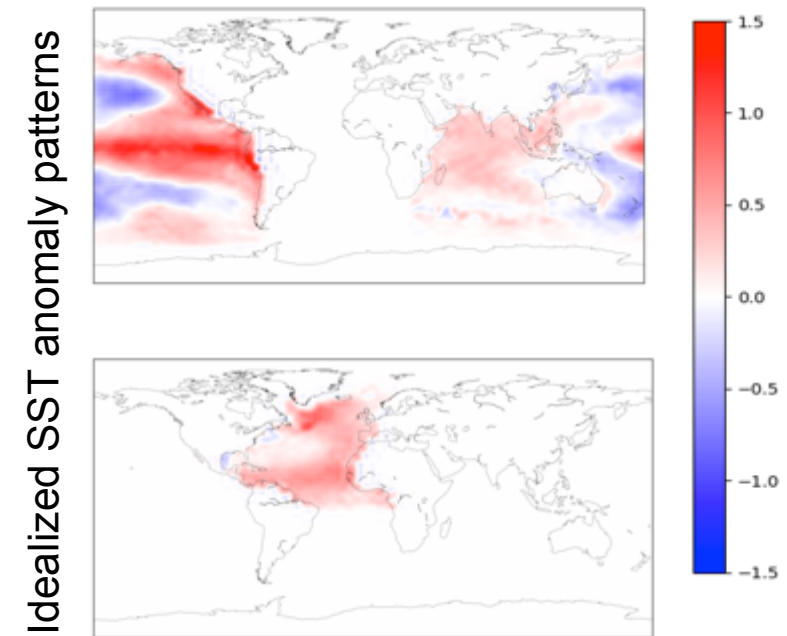
	Atlantic	Warm	Neutral	Cold
Pacific				
Warm		PwAw	PwAn	PwAc
Neutral		PnAw	PnAn	PnAc
Cold		PcAw	PcAn	PcAc

Model	Resolution	Reference
✓ AM2.1 GFDL	2×2.5, L25	Delworth et al. (2006)
GFS	T62 (~2×2), L64	Campana and Kaplan (2005)
✓ NSIPP-1	3×3.75, L34	Bacmeister et al. (2000)
CCM3.0	T42 (~2.8×2.8), 18 hybrid levels	Kiehl et al. (1998)
✓ CAM3.5	T85, 27 hybrid levels Reference	Collins et al. (2006), Neale et al. (2008)

Total Runoff Integrating Pathways (TRIP) network (Oki and Sud 1998)

The **aim of TRIP** is to provide information of lateral water movement over land following the paths of river channels.

Assumed input to TRIP is runoff from global land models, and output is discharge data prepared at **1 latitude 1 longitude** resolution.



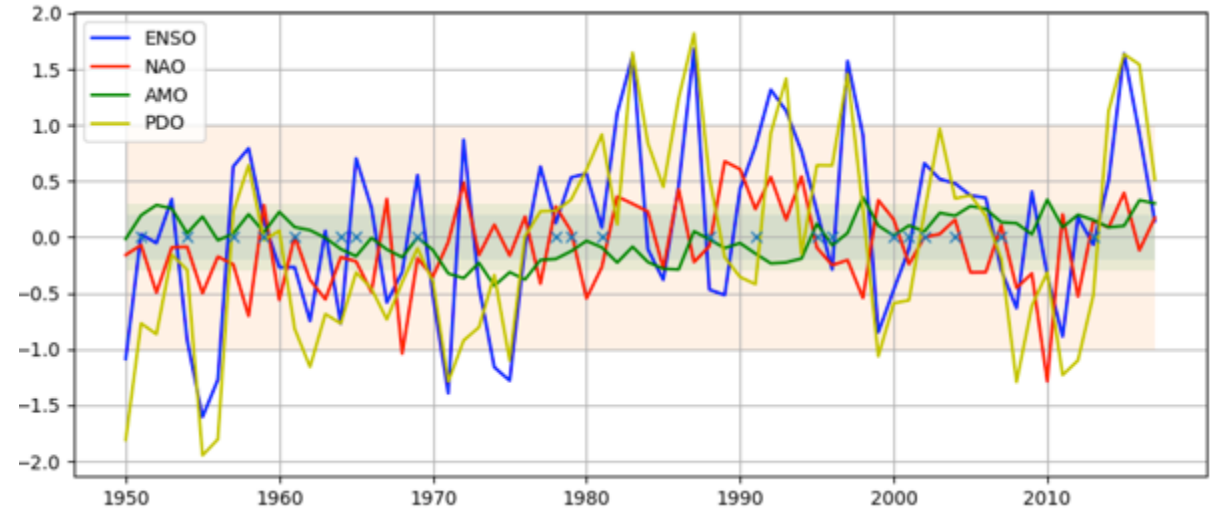
Validation

➤ : Neutral Year selection

The PDO, ENSO, NAO and AMO(unsmoothed) index from 1950 to 2017 were collected ; the neutral year was defined as when

$$-1 < \text{PDO} < 1 \ \& \ -1 < \text{ENSO} < 1 \ \& \ -0.3 < \text{NAO} < 0.3 \ \& \ -0.2 < \text{AMO} < 0.2$$

As the result , 22 years were selected as neutral years.*

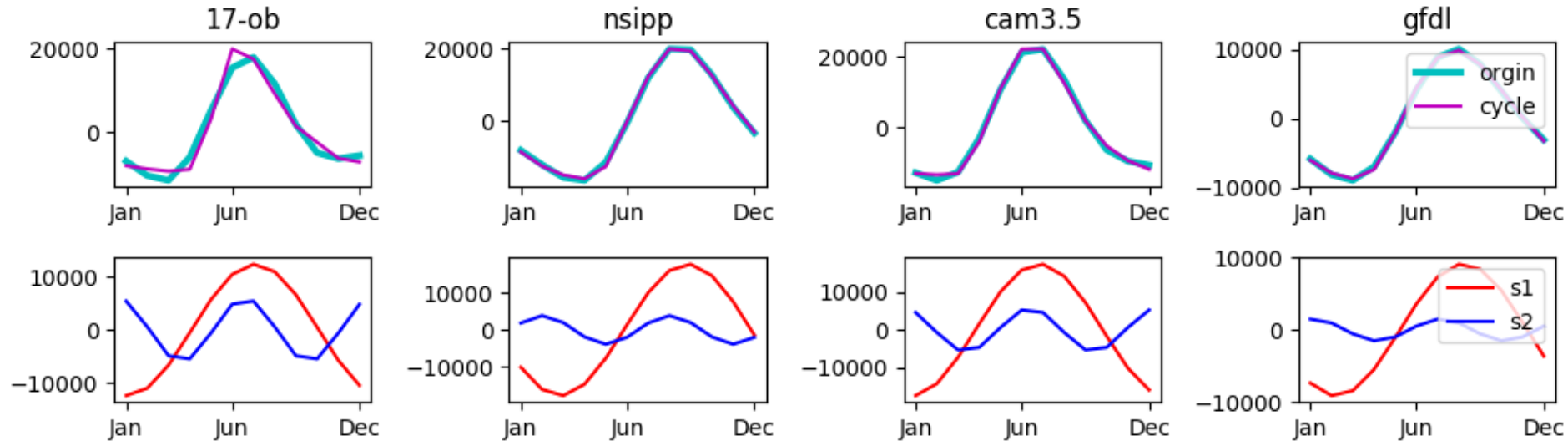


➤ : Harmonic Analysis :

The discharge of all target rivers of the corresponded Neutral year were collected, averaged and standardized to get 12 months discharge variation. So are the PnAn scenario of all three models.

- Enfield, D.B., A.M. Mestas-Nunez, and P.J. Trimble, 2001: The Atlantic Multidecadal Oscillation and its relationship to rainfall and river flows in the continental U.S., *Geophys. Res. Lett.*, 28: 2077-2080.
- Wolter, K., and M.S. Timlin, 1998: Measuring the strength of ENSO - how does 1997/98 rank? *Weather*, 53, 315-324.
- Hurrell, J.W., 1995: Decadal trends in the North Atlantic Oscillation and relationships to regional temperature and precipitation. *Science* 269, 676-679.

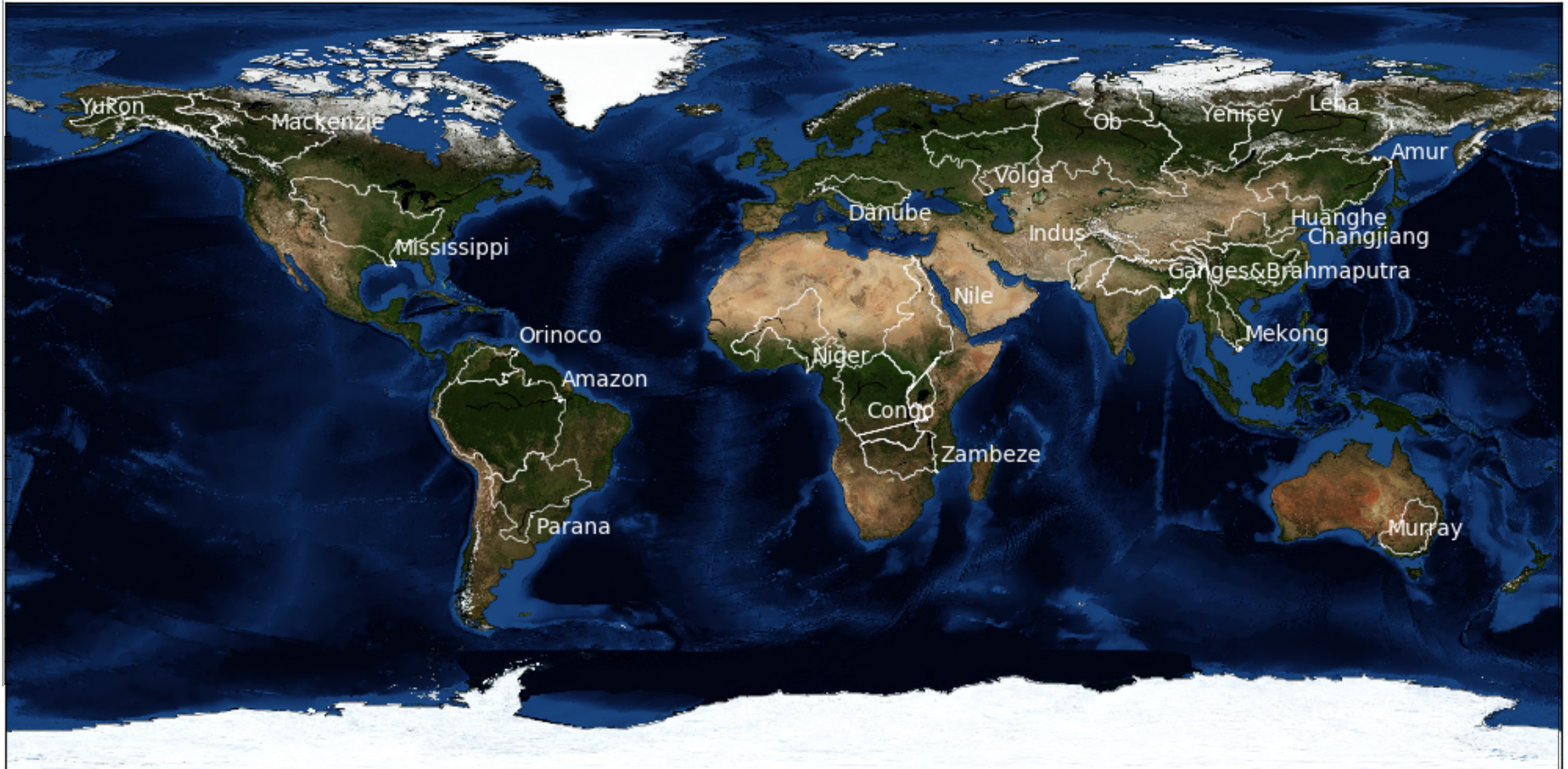
The harmonic analysis was applied and the correlation coefficient (R) was calculated between observation and each of the three models , with models whose R lower than 0.7 are discarded



* Including the year 1951, 1954, 1957, 1959, 1961, 1964, 1965, 1969, 1978, 1979, 1981, 1988, 1991, 1995, 1996, 2000, 2001, 2002, 2004, 2007, 2013

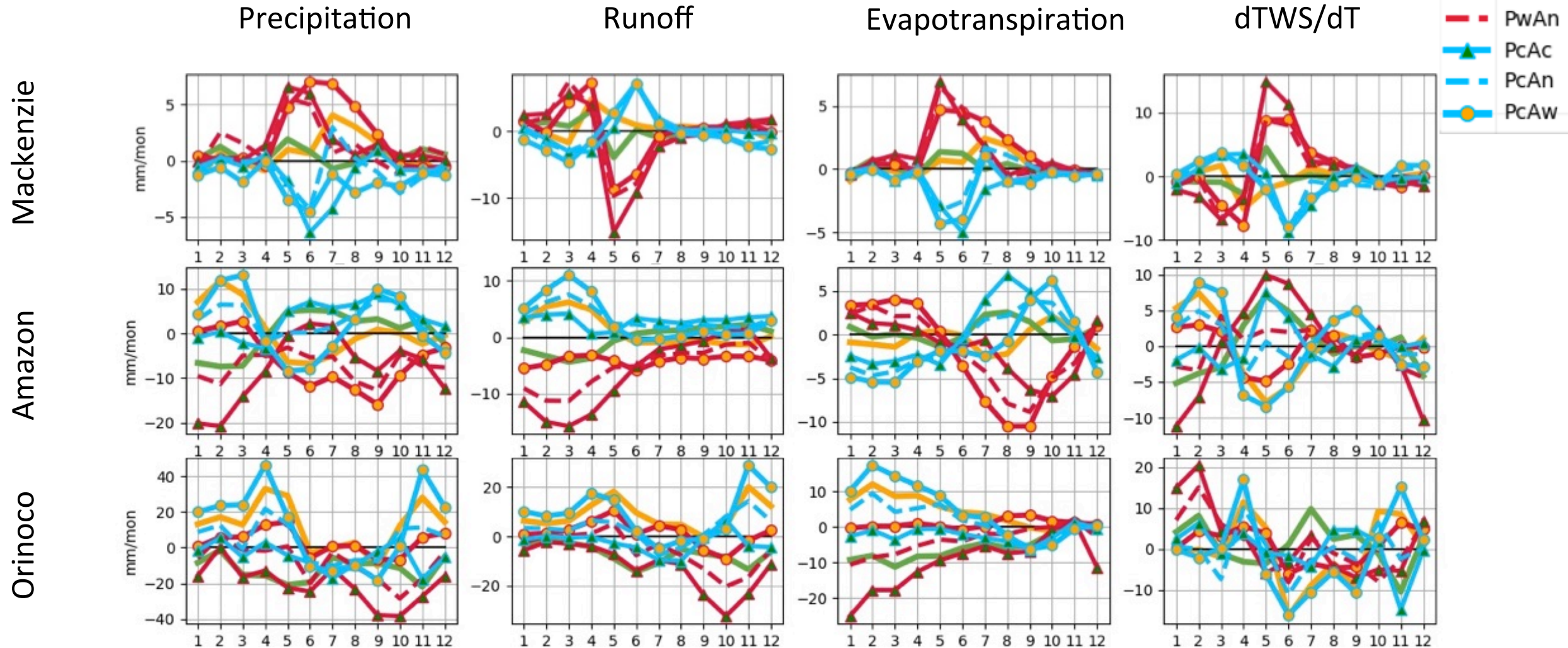
23 target river basins

Covers: 40% of global ocean-draining land; Drainage Area = $40.41 \times 10^6 \text{ km}^2$



Analysis

The selected ($R > 0.7$) river basins and corresponded models are further analyzed on seasonal scale, the Mackenzie river, Orinoco and Amazon river basin are shown as examples:



> y-axis denotes basin-wide average value of each scenario's difference from neutral scenario, that is $(P_x A_x - P_n A_n)$

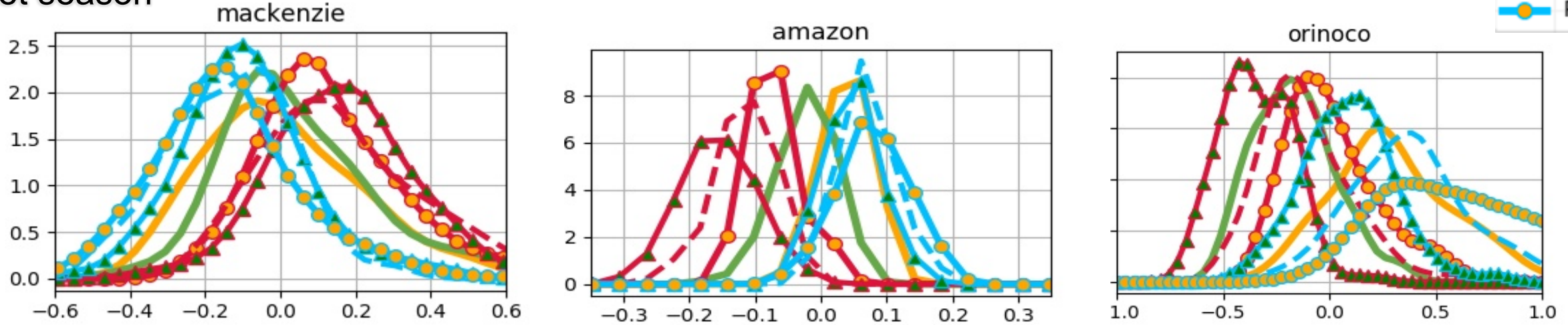
> dTWS/dT was calculated using $dTWS/dT = P - ET - R$

Analysis

- >For each target river, the 3-months dry season and wet season are identified from Observation data;
- >The kernel density estimation (KDE) is applied to estimate the probability density function (PDF) of relative discharge variation of each scenarios $((P_{xAx}-P_{nAn})/P_{nAn})$ for its dry season and wet season respectively



Wet season



Mackenzie

- >robust response to SST anomalies at its wet season;
- >PwAc creating nearly 20% more discharge while PcAw symmetrically 20% less discharge;
- >Pacific Ocean has a dominating role in here

Amazon

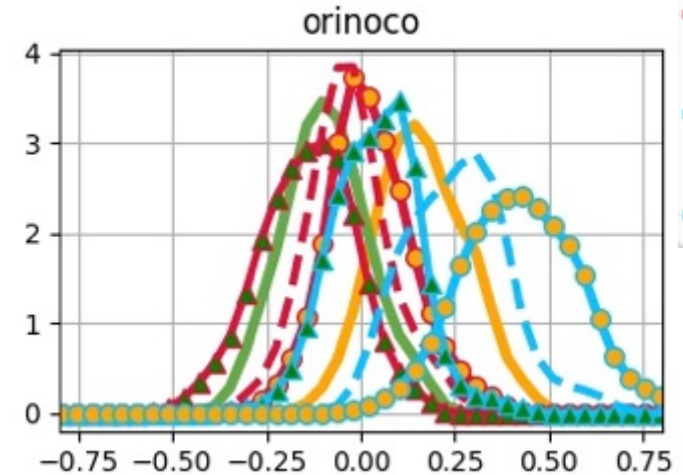
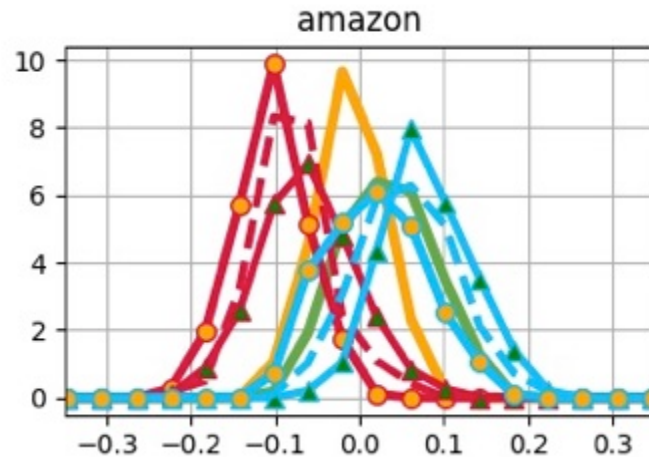
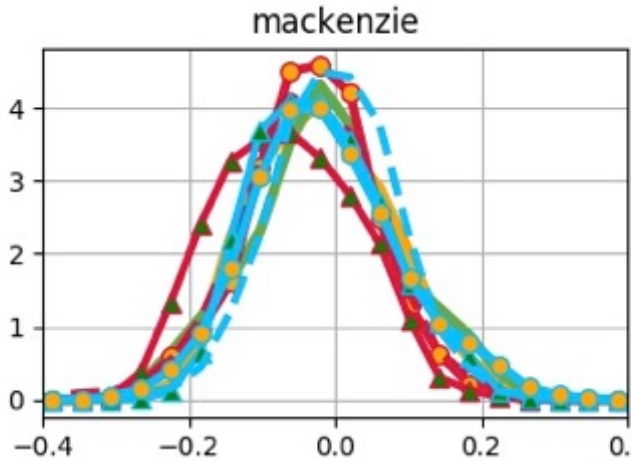
- >the largest response of Amazon river discharge variations tends to occur when the two oceans have anomalies of opposite signs;
- >Pacific warm has stronger impact on discharge than cold scenario;

Orinoco

- >Resembles Amazon's pattern, with overall Atlantic shows more strength influence discharge change, Atlantic warm alone (PnAw) cause 25% more discharge at wet season

Analysis

dry season



Mackenzie :

- > SST has relatively moderate influence on its dry season;
- > PwAc averagely reduced discharge by 10%

Amazon :

- > When the two oceans are forced with the same signal (PwAw or PcAc) , the PDFs has the largest response (conform with J.-H. Yoon 2016)
- > Pw - overall drier condition
- > Pc - overall wetter condition
- > similar to the dry season, discharge shows slight robust response to Pacific warm than to Pacific cold sign;

Orinoco

- > Resemble its wet season pattern , with PwAc curves shift to the right by around 30%

Conclusions

- Pacific SST anomaly is dominating pattern of the basin-wide hydrology changes across the globe; Pacific warm's (resembles El Nino) influence on rivers has overall higher amplitude than Pacific cold (resembles La Nina) ;
- There is general agreement among the Rivers that the largest extreme tends to occur when the two oceans have anomalies of opposite signs;
- SST forcings show difference influence on rivers across seasons, for example, Amazon river with Pw induced evapotranspiration higher than neutral condition for the first half year, but lower than neutral for the second half year.

**THANK YOU
FOR
YOUR ATTENTION**

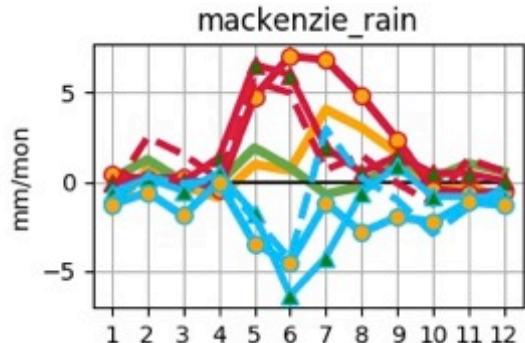
Appendix

River_Name	J	F	M	A	M	J	J	A	S	O	N	D
Amazon					Wet	Wet	Wet			Dry	Dry	Dry
Amur	Dry	Dry	Dry				Wet	Wet	Wet			
Brahmaputra			Dry					Wet	Wet			
Congo	Wet						Dry	Dry	Dry		Wet	Wet
Danube				Wet	Wet	Wet		Dry	Dry	Dry	Dry	
Ganges			Dry	Dry	Dry		Wet	Wet	Wet			
Indus	Dry	Dry					Wet	Wet	Wet			Dry
Lena		Dry	Dry	Dry		Wet	Wet	Wet				
Mackenzie		Dry	Dry	Dry		Wet	Wet	Wet				
Mekong		Dry	Dry	Dry				Wet	Wet	Wet		
Mississippi			Wet	Wet	Wet			Dry	Dry	Dry		
Murray		Dry	Dry	Dry				Wet	Wet	Wet	Wet	
Niger			Dry	Dry	Dry			Wet	Wet	Wet		
Nile			Dry	Dry	Dry	Wet	Wet	Wet				
Ob		Dry	Dry	Dry		Wet	Wet	Wet				
Orinoco		Dry	Dry	Dry			Wet	Wet	Wet			
Parana			Wet	Wet	Wet			Dry	Dry	Dry		
Yangtze	Dry	Dry				Wet	Wet	Wet				Dry
Yellow	Dry	Dry	Dry					Wet	Wet	Wet		
Yenisey	Dry	Dry			Wet	Wet	Wet					Dry
Zambezi			Wet	Wet	Wet				Dry	Dry	Dry	
Yukon	Dry	Dry	Dry			Wet	Wet	Wet				
Volga	Dry			Wet	Wet	Wet					Dry	Dry

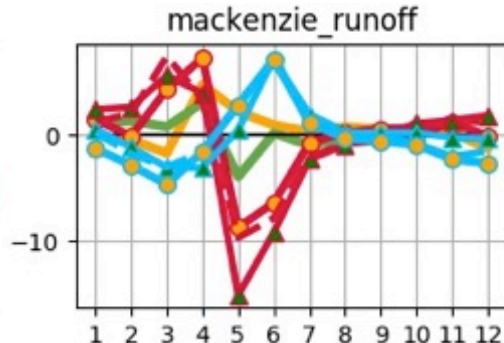
Index:	
Wet Season	Wet
Dry Season	Dry

Mackenzie

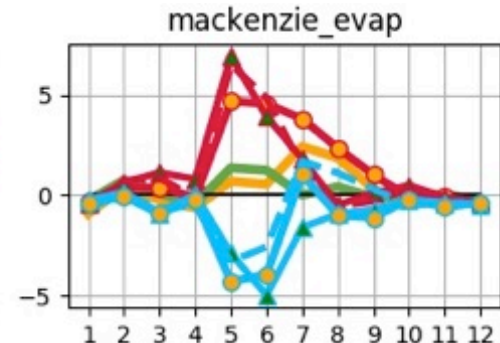
Precipitation



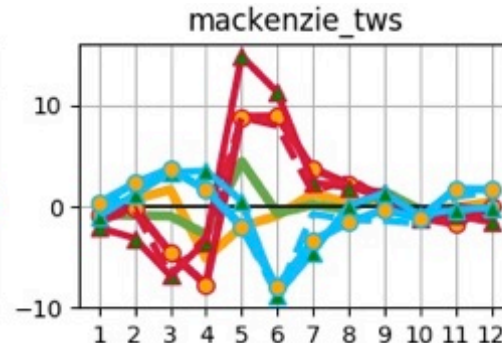
Runoff



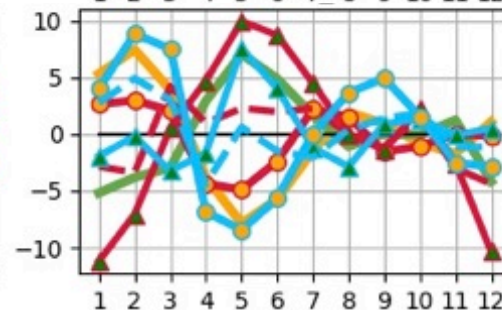
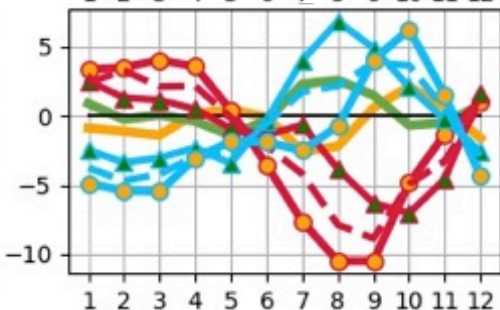
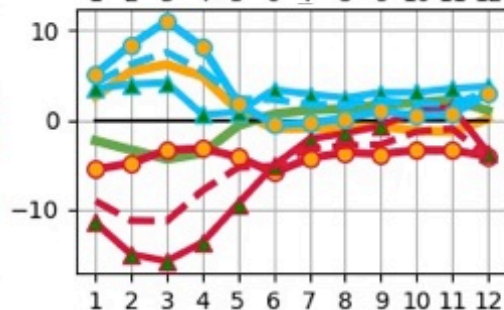
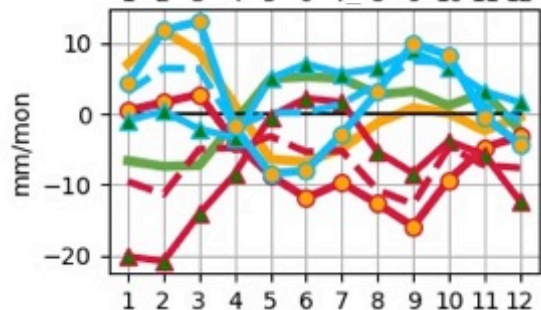
Evapotranspiration



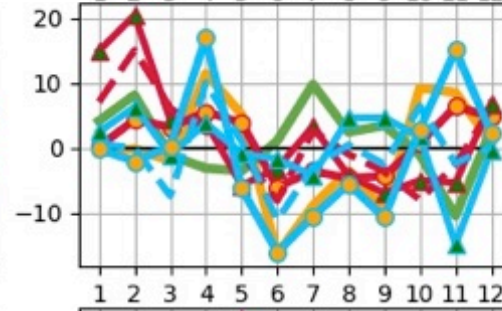
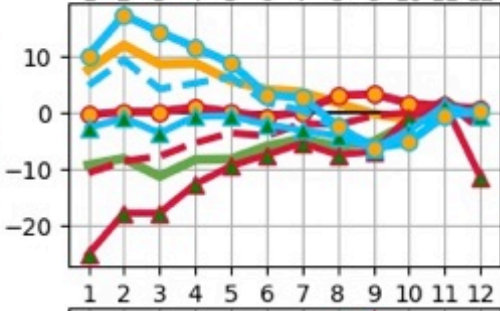
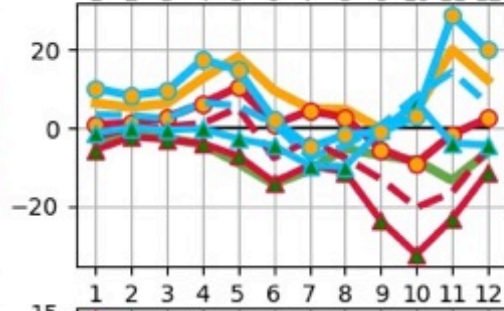
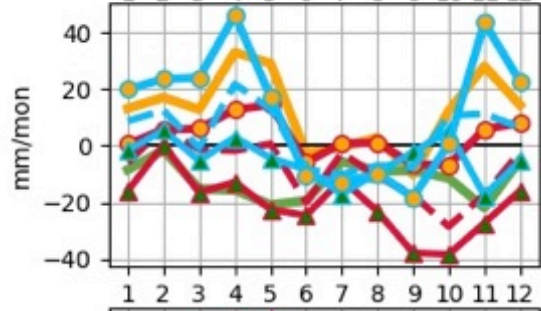
dTWS/dT



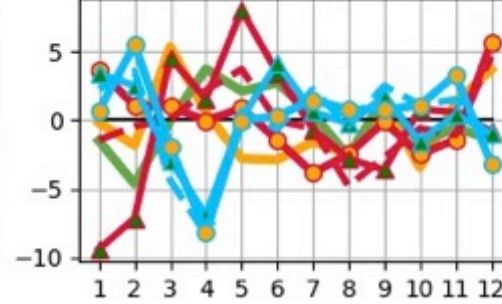
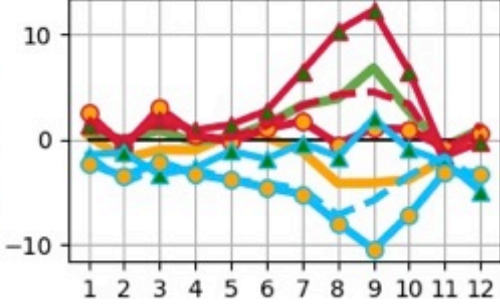
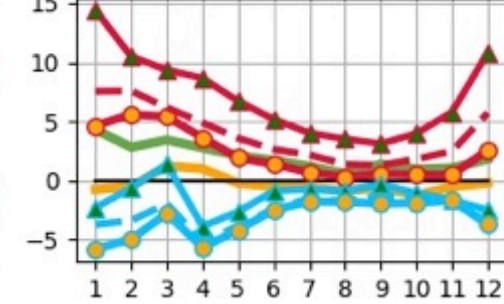
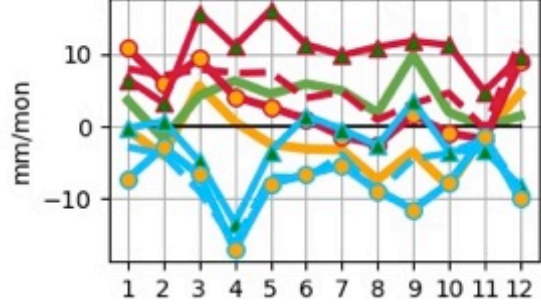
Amazon



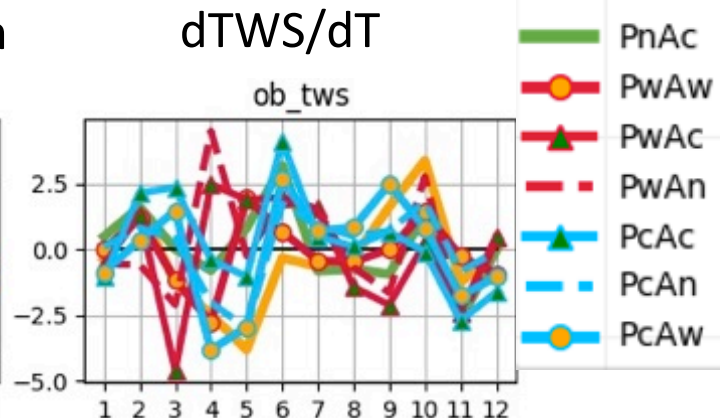
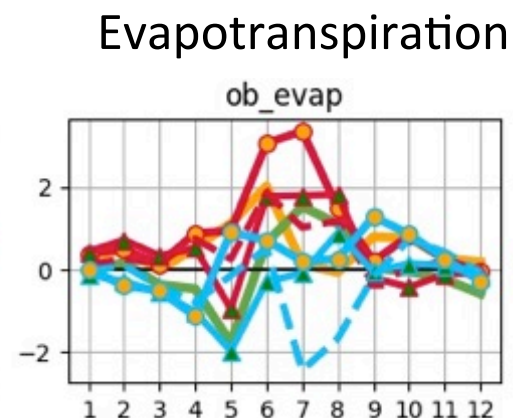
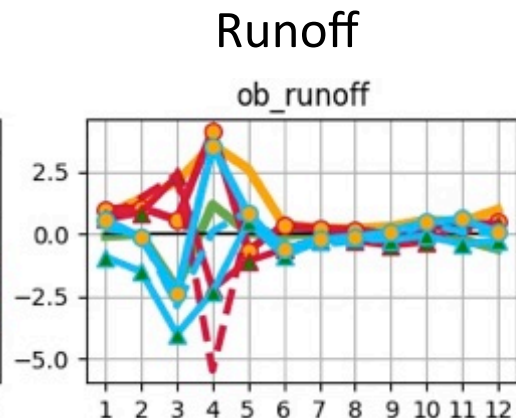
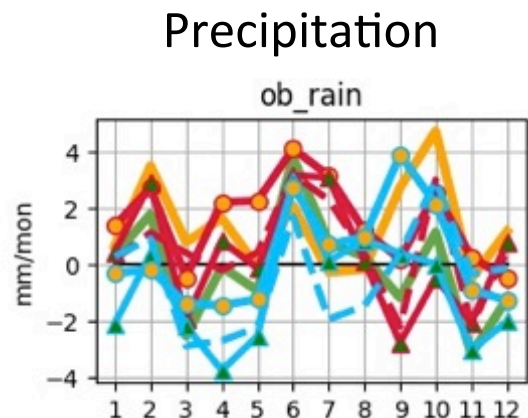
Orinoco



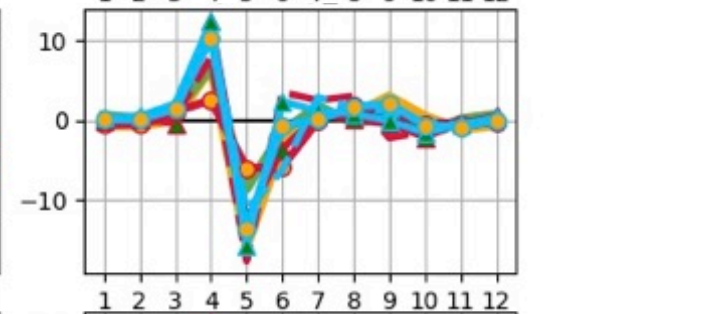
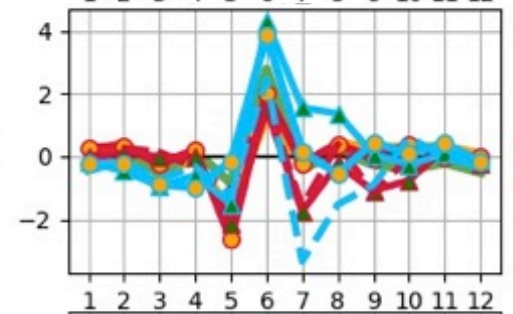
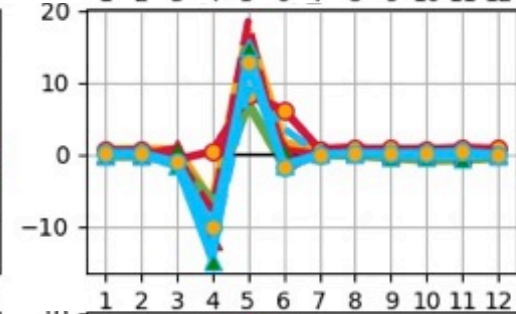
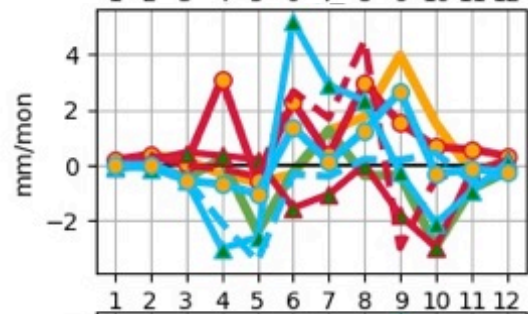
Parana



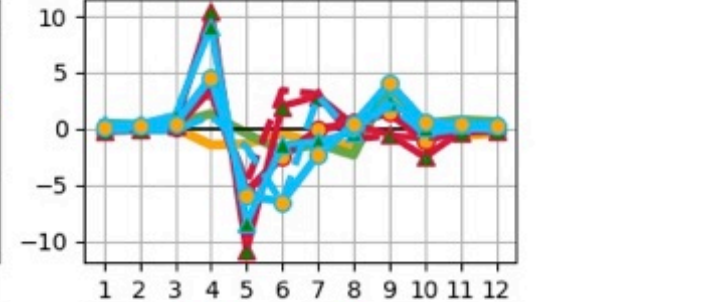
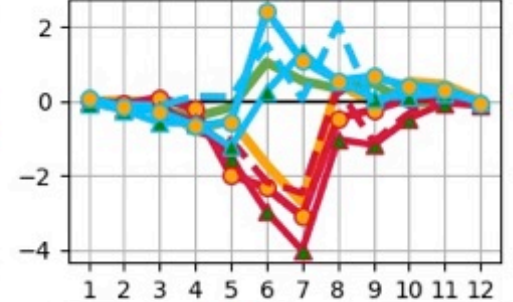
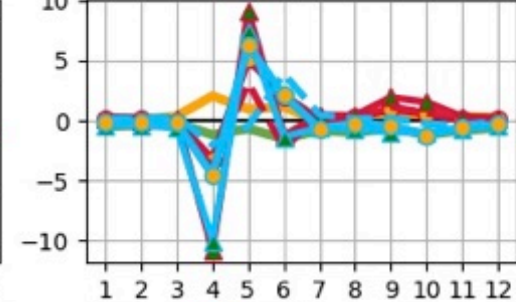
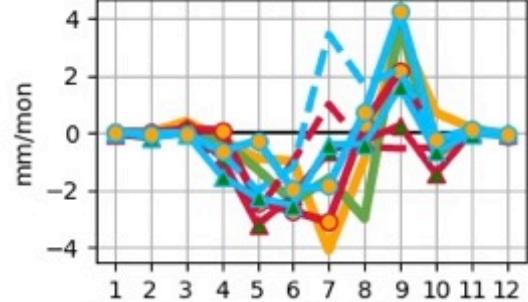
Ob



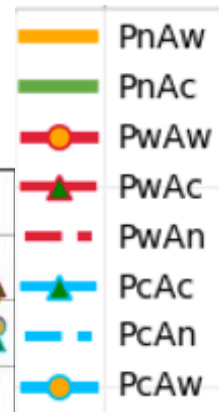
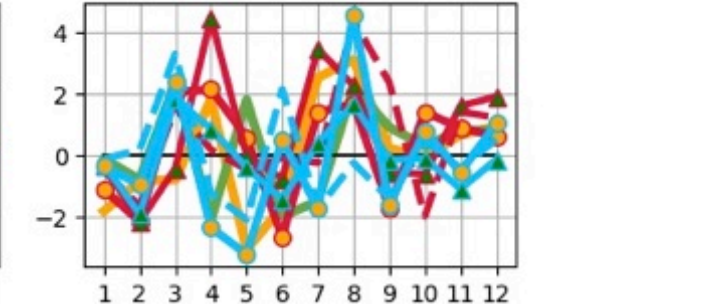
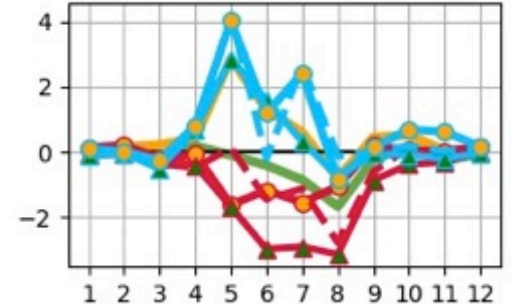
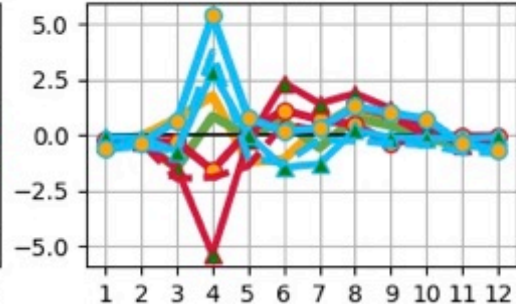
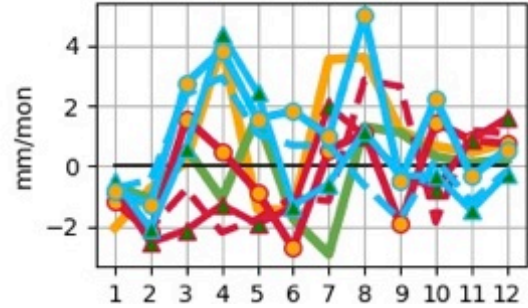
Yenisei



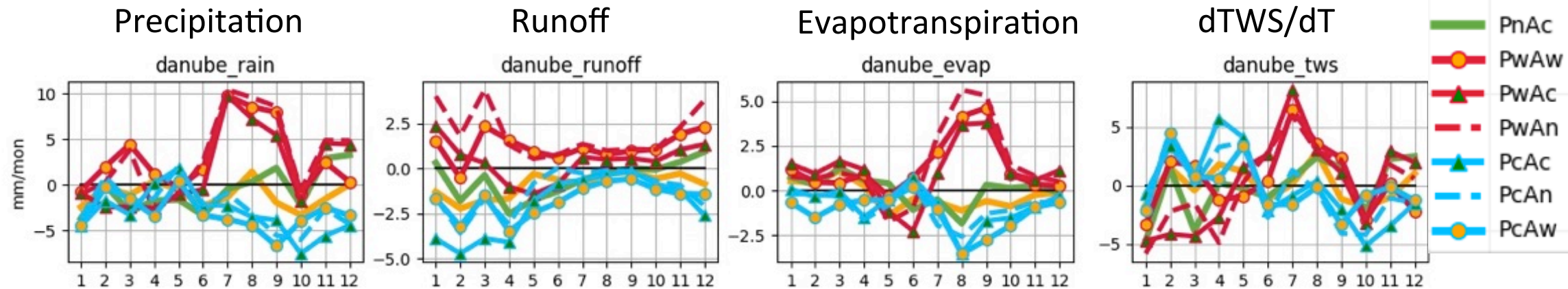
Lena



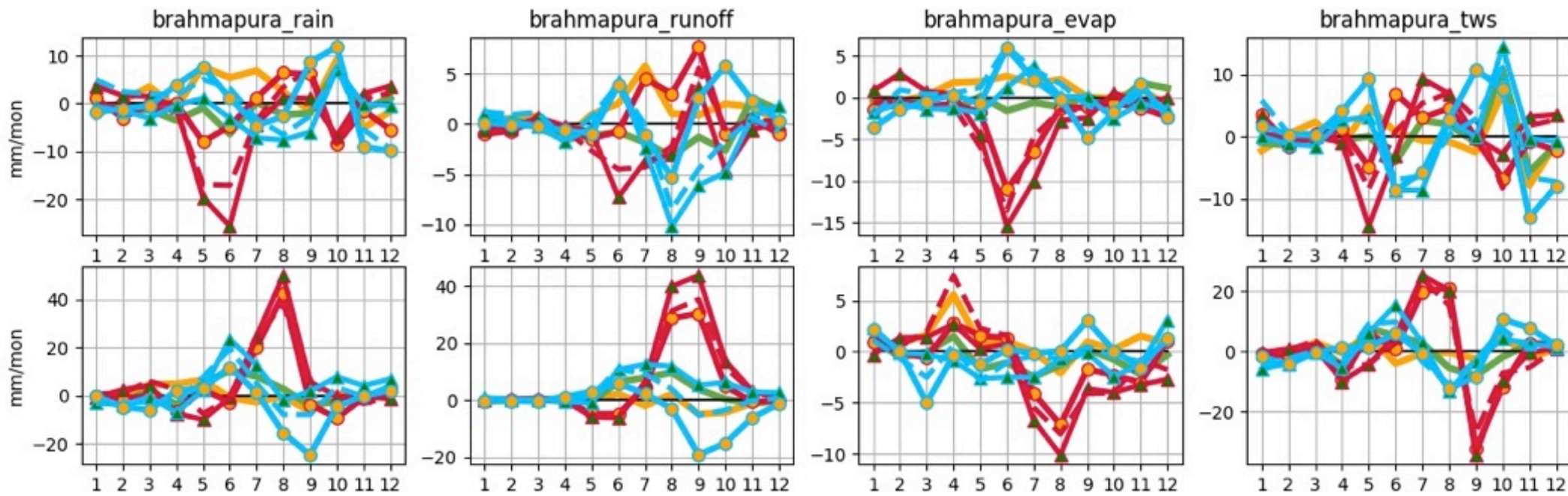
Amur



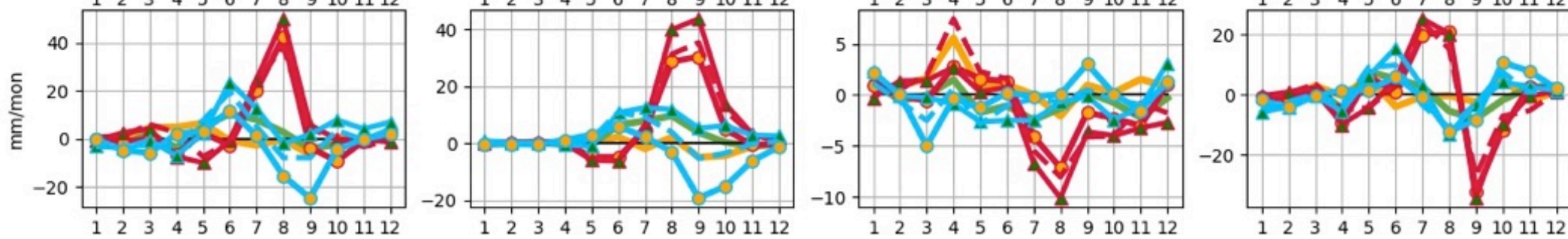
Danube



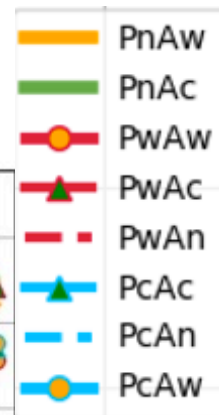
Zambezi



G&B



Mekong

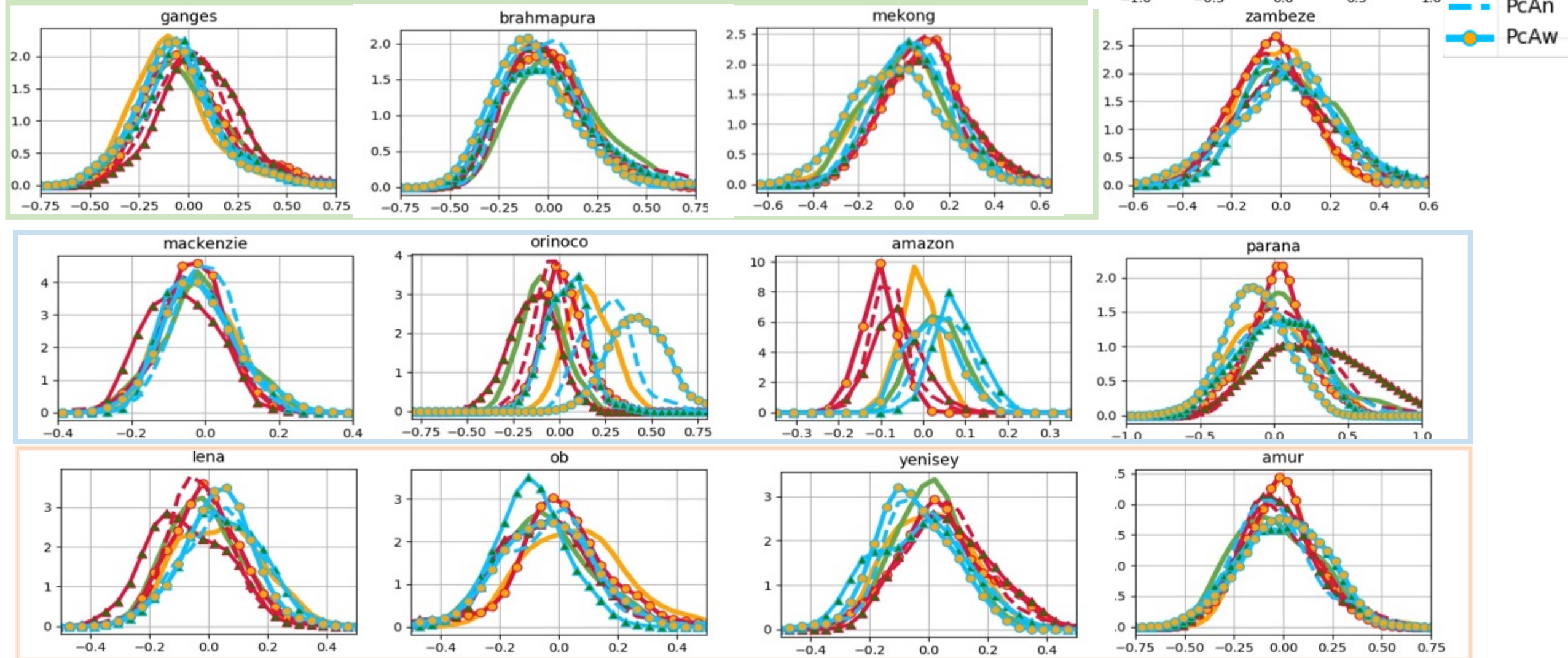


>For each target river, the 3-months dry season and wet season are identified from Observation data;

>The kernel density estimation (KDE) is applied to estimate the probability density function (PDF) of relative discharge variation of each scenarios ((PxAx-PnAn)/PnAn)for its dry season and wet season respectively

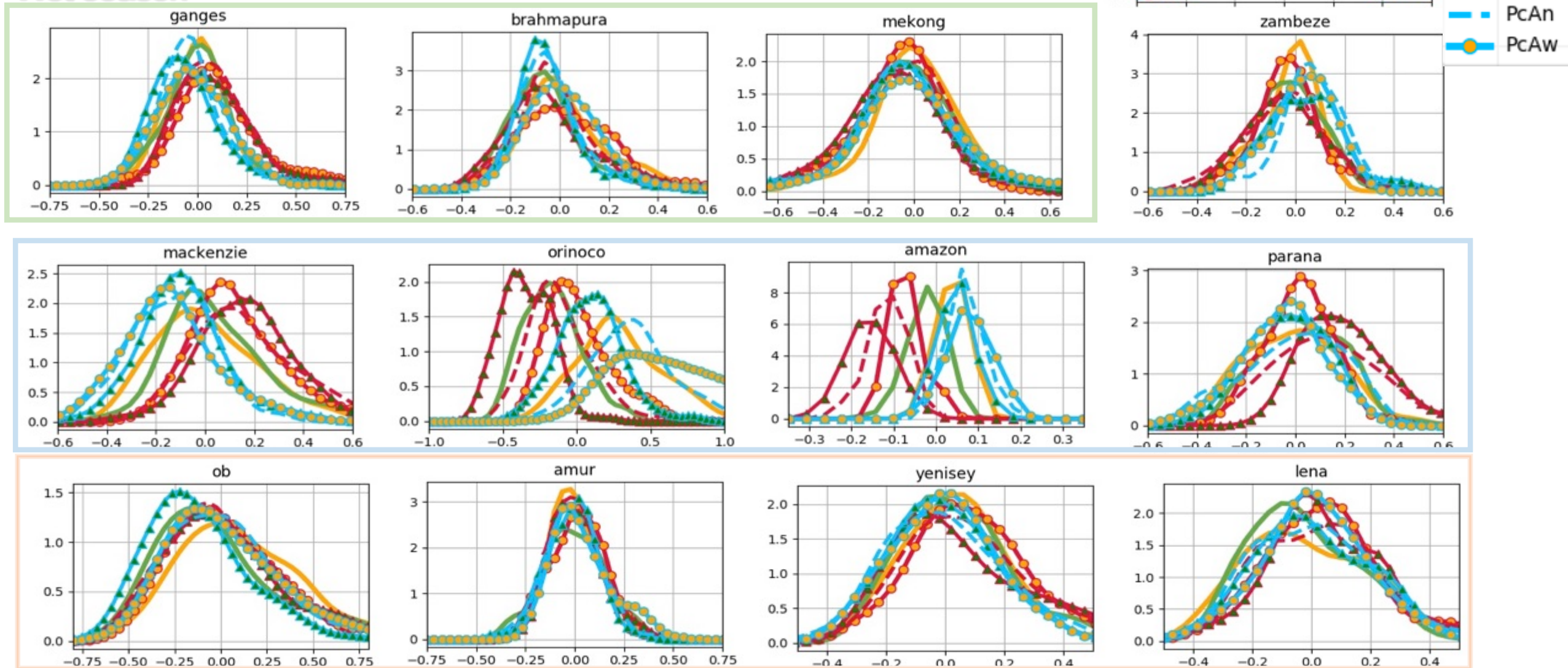
dry season

South Asia America North Asia



> Rivers in the American continent show robust shift of PDF for both Pacific and Atlantic signals, with PcAW
>

Wet season



(1, 0.73526711879150575, 0.97532497267477514, 0.75571507822754658)
(1, 'n=', 1, 'c=', 1, 'g=', 1)
(2, 0.73023514036873938, 0.84918564837846788, 0.40474975188783474)
(2, 'n=', 1, 'c=', 1, 'g=', 0)
(3, 0.92530402023666647, 0.59471020782445094, 0.69261282728371809)
(3, 'n=', 1, 'c=', 0, 'g=', 1)
(4, -0.15985562723397423, -0.37817264953973317, -0.3064984219138977)
(5, -0.69443517084470752, -0.4235380752372046, -0.8967186328553628)
(6, 0.91681652583231688, 0.90299182087707064, 0.89438076774266362)
(6, 'n=', 1, 'c=', 1, 'g=', 1)
(7, 0.75974092060213272, 0.6660510737198263, 0.83242410426291891)
(7, 'n=', 1, 'c=', 0, 'g=', 1)
(8, -0.080598655512610945, 0.22897241710178465, 0.19107825392154376)
(9, 0.30286608358657491, 0.48498185377790071, 0.19567940997685832)
(10, -0.15042370131658894, 0.69774195347459533, -0.33412302850307141)
(10, 'n=', 0, 'c=', 1, 'g=', 0)
(11, 0.54055410784812818, 0.97766655706307348, 0.80119298157355889)
(11, 'n=', 0, 'c=', 1, 'g=', 1)
(12, 0.4760413787517711, 0.77670729385554393, 0.81707274649729922)
(12, 'n=', 0, 'c=', 1, 'g=', 1)
(13, -0.96270903995107193, 0.27668240347516554, -0.29740519915441332)
(14, -0.7347721313956751, -0.80884158950396079, -0.27758442392693844)
(15, 0.28593839108984931, -0.11195534697380302, 0.52935296699727619)
(16, -0.42821781289356919, -0.34675050602457808, 0.039986229428484857)
(17, 0.53582779594533891, 0.98049943449756216, 0.79367991072937494)
(17, 'n=', 0, 'c=', 1, 'g=', 1)
(18, 0.48771664588388319, 0.73679469883741733, 0.25857712253815646)
(18, 'n=', 0, 'c=', 1, 'g=', 0)
(19, 0.66254973701570952, 0.81217686606965145, 0.25835737251010954)
(19, 'n=', 0, 'c=', 1, 'g=', 0)
(20, -0.10212968717770178, 0.69953105286945017, 0.066950285759401845)
(20, 'n=', 0, 'c=', 1, 'g=', 0)
(21, 0.97388812629495025, 0.92905624938124687, 0.9700176373777607)
(21, 'n=', 1, 'c=', 1, 'g=', 1)
(22, 0.46173309400802681, 0.56319866570022348, 0.0074604602237468469)
(23, -0.51754208109427302, 0.36407410926091882, 0.48535538869046785)

No	River_Name
1	Amazon
2	Amur
3	Brahmaputra
4	Changjiang
5	Congo
6	Danube
7	Ganges
8	Huanghe
9	Indus
10	Lena
11	Mackenzie
12	Mekong
13	Mississippi
14	Murray
15	Niger
16	Nile
17	Ob
18	Orinoco
19	Parana
20	Yenisey
21	Zambeze
22	Yukon
23	Volga